

# Effects of $\beta$ -Cyclodextrin on the Structure of Sphingomyelin/Cholesterol Model Membranes

Michael S. Jablin,<sup>†</sup> Michał Flasiński,<sup>‡</sup> Manish Dubey,<sup>†</sup> Dilru R. Ratnaweera,<sup>§</sup> Marcin Broniatowski,<sup>‡</sup> Patrycja Dynarowicz-Łątka,<sup>‡</sup> and Jarosław Majewski<sup>†\*</sup>

<sup>†</sup>Lujan Neutron Scattering Center, Los Alamos National Laboratory, Los Alamos, New Mexico; <sup>‡</sup>Jagiellonian University, Faculty of Chemistry, Kraków, Poland; and <sup>§</sup>Department of Chemistry, Clemson University, Clemson, South Carolina

**ABSTRACT** The interaction of  $\beta$ -cyclodextrin ( $\beta$ -CD) with mixed bilayers composed of sphingomyelin and cholesterol (Chol) above and below the accepted stable complexation ratio (67:33) was investigated. Membranes with the same (symmetric) and different (asymmetric) compositions in their inner and outer leaflets were deposited at surface pressures of 20, 30, and 40 mN/m at the solid-liquid interface. Using neutron reflectometry, membranes of various global molar ratios (defined as the sum of the molar ratios of the inner and outer leaflets), were characterized before and after  $\beta$ -CD was added to the subphase. The structure of bilayers with global molar ratios at or above the stable complexation ratio was unchanged by  $\beta$ -CD, indicating that  $\beta$ -CD is unable to remove sphingomyelin or complexed Chol. However,  $\beta$ -CD removed all uncomplexed Chol from bilayers composed of global molar ratios below the stable complexation ratio. The removal of Chol by  $\beta$ -CD was independent of the initial structure of the membranes as deposited, suggesting that asymmetric membranes homogenize by the exchange of molecules between leaflets. The interaction of  $\beta$ -CD with the aforementioned membranes was independent of the deposition surface pressure except for a symmetric 50:50 membrane deposited at 40 mN/m. The scattering from 50:50 bilayers with higher packing densities (deposited at 40 mN/m) was unaffected by  $\beta$ -CD, suggesting that the removal of Chol can depend on both the composition and packing density of the membrane.

## INTRODUCTION

The fluid mosaic model for cell membranes has served as a fundamental construct in membrane biology for over 30 years (1). According to this model, cellular membranes are in the disordered fluid state, characterized by a random distribution of their components, and are composed of a variety of lipids and proteins that experience both rotational and translational freedom within the bilayer plane (2). More recent detailed studies have shown that lipids are not only distributed asymmetrically between the biomembrane leaflets (3,4) but also dispersed heterogeneously within a single layer. It is accepted that cellular membranes contain stable, highly ordered microstructures, so-called lipid rafts, which display physicochemical properties different from those of their disordered fluid surroundings. The term lipid raft (5) was coined for closely packed, small (100 to 2000 Å) domains enriched in cholesterol (Chol) and sphingolipids, for which subsequent research identified the stable complexation ratio to be 67:33 (sphingomyelin (SM)/Chol) (6,7). Further research indicated the significant role of lipid rafts in many important cellular processes, such as signal transduction and trafficking (8–10), sorting of lipids and proteins (8–11), and mitigation of viral and bacterial infections (12,13).

Lipid rafts are resistant to some surfactants, which are able to disturb the less organized domains of biomembranes but are unable to lyse rafts (14). The durability of lipid rafts makes it possible to isolate them from membranes and

subsequently identify them (15,16). After isolation, experiments can be performed to elucidate the specific interactions between lipid rafts and different agents that have known effects on disordered biomembrane domains. Cyclodextrins (CDs) are among the substances that can profoundly modify the structure and function of biomembranes, and they have been the object of intensive study in recent years (17–19). These macrocycles belong to a class of cyclic oligosaccharides consisting of several glucose units linked together by  $\alpha$ -1,4-glucosidic bonds. Three major representatives— $\alpha$ -,  $\beta$ -, and  $\gamma$ -CD—contain six, seven, and eight glucopyranose units, respectively, in their molecules. The external surface of the CD toroid is hydrophilic, whereas its cavity possesses a nonpolar character. It has been well established that CDs are able to form inclusion complexes with a wide variety of organic guests: molecules, ions, or even radicals. The complexation of a guest molecule (or its part) takes place by either partially or totally filling the CD hydrophobic cavity (20). The interaction of CDs with different model membranes has been thoroughly investigated (21,22). The removal of Chol from lipid membranes using  $\beta$ -CD established that this substance has appropriate molecular dimensions to form inclusion complexes with sterol molecules. In contrast, CDs are unable to complex double-chained phospholipids, since their cross-sectional area exceeds the dimensions of the CD cavity (16,23). Many investigations of  $\beta$ -CD/membrane interactions have involved cell lines (17,24,25), lipid vesicles (18,26–28), and one-component sterol monolayers (19,29). Although some studies suggest that  $\beta$ -CD can affect double-chain lipids (phosphocholine

Submitted April 6, 2010, and accepted for publication June 14, 2010.

\*Correspondence: jarek@lanl.gov

Editor: Thomas J. McIntosh.

© 2010 by the Biophysical Society  
0006-3495/10/09/1475/7 \$2.00

doi: 10.1016/j.bpj.2010.06.028

and SM) (28,30,31), in other studies no effect is observed (26,32). However, there is general agreement that in the presence of SM,  $\beta$ -CD removes less Chol at a diminished rate compared to the case for Chol/phosphocholine systems. This phenomenon has been studied using large unilamellar vesicles and erythrocyte ghosts (26), small unilamellar vesicles (27), and monolayers (32).

Previous studies have used  $\beta$ -CD to remove Chol from cellular membranes (17,24,25) to investigate the effect of Chol depletion on cell viability and functionality. These studies commonly involve cultured cells where Chol is present not only in the cell membrane but also in intracellular stores. When  $\beta$ -CD removes Chol from the plasma membrane, the Chol can be replenished from these stores. Thus, the effect of  $\beta$ -CD on the structure of the membrane is difficult to assess. Ohvo-Rekila et al. emphasize the importance of focused model membrane experiments to decipher biological reality (22). In our study, we investigated the interaction of  $\beta$ -CD with mixed SM/Chol bilayers in which the amount of Chol is controlled. To this end, we created model membranes consisting of varying molar ratios of SM and Chol above and below the accepted stable complexation ratio (67:33). The SM/Chol bilayers were characterized by neutron reflectometry (NR) before and after the introduction of  $\beta$ -CD. Our objectives were to probe the influence of  $\beta$ -CD on the structure, composition, and reorganization of mixed SM/Chol bilayers. To our knowledge, these are the first neutron scattering studies of interactions between  $\beta$ -CD and mixed SM/Chol bilayers.

## MATERIALS AND METHODS

### Sample preparation

SM derived from chicken egg, Chol derived from ovine wool, and deuterated Chol (dChol, in which seven hydrogen atoms are replaced by deuterium atoms) were purchased from Avanti Polar Lipids (Alabaster, AL) and used without further purification. Stock solutions of both compounds were prepared by dissolving chemicals in chloroform and methanol and then mixing to create various molar ratios of SM/Chol: 100:0, 90:10, 67:33, 50:50, and 33:67. Complete bilayers with molar ratios below 33:67 could not be created, providing additional evidence that Chol precipitates from membranes with a proportion of Chol beyond 33:67 (33). Membrane depositions were completed in a clean room where the temperature was maintained at  $23 \pm 2^\circ\text{C}$ . The mixed solutions were deposited by a microsyringe onto the air/water interface in a Langmuir trough (NIMA, Coventry, United Kingdom). At least 10 min were allowed for solvent evaporation, after which time the monolayers were compressed to 20, 30, or 40 mN/m. At room temperature and surface pressures  $\geq 20$  mN/m, the monolayers of SM and Chol are in the gel phase (34). After film stabilization, the inner and outer membrane leaflets were transferred by the Langmuir-Blodgett (LB) and Langmuir-Schaefer (LS) techniques, respectively, onto quartz monocrystals 3 in in diameter (c-cut, alpha quartz, density  $2.64\text{--}2.65\text{ g cm}^{-3}$ , Institute of Electronic Materials Technology, Warsaw, Poland). Before depositing the lipids, the quartz substrates were cleaned thoroughly by rinses alternating between chloroform, toluene, methanol, and high-purity (18 M $\Omega$ ) water. Finally, the substrates were placed in an ultraviolet-ozone cleaner for 20 min. Although it is more common to create membranes in which the inner and outer leaflets contain the same compo-

sition (symmetric), it is possible to create membranes where the composition of the two leaflets is initially different (asymmetric). Both of these types of membranes were created to investigate the effect of starting membrane structure on its interaction with  $\beta$ -CD. We categorize membranes according to their global molar ratio, which is defined as the sum of the molar ratios of the two leaflets. For example, a membrane with an inner leaflet composed of 33:67 and an outer leaflet of 67:33 (sum = 100:100) is categorized as a 50:50 global molar ratio membrane.

The bilayers were measured in a solid-liquid interface cell (Fig. S1 in the Supporting Material) at room temperature. The setup was composed of a quartz substrate supported by an O-ring and a Macor ceramic disk (Ceramic Products, Palisade Park, NJ). The Macor, O-ring, and substrate define a reservoir 0.2 to 0.3 mm thick for the subphase. The entire sample environment was held in place with aluminum clamps. Neutrons entered the lateral face of the quartz substrate and were scattered from the quartz-subphase interface. The bilayers were first characterized against a subphase of D<sub>2</sub>O before injecting a 1 mM solution of  $\beta$ -CD (Fisher Scientific, Pittsburgh, PA) into the reservoir of the solid-liquid cell. D<sub>2</sub>O provides neutron scattering contrast between quartz, the hydrogen-rich bilayer, and the subphase.

### Neutron reflectometry

NR is an excellent tool to study in situ the structure of thin hydrogenated films at the solid-liquid interfaces. Neutrons are sensitive to the scattering contrast between a hydrogenated layer and a deuterated subphase. If any of the deuterated subphase is incorporated into the hydrogenated layer, the scattering contrast between the layer and the subphase will change. The change in contrast will be immediately apparent in the scattering from the system. In our case, NR can be used to directly assess the amount of material removed from mixed SM/Chol bilayers. Removal of material can result in membrane reorganization, which could be followed by the incorporation of the deuterated subphase into regions no longer occupied by membrane. In addition, unlike x-ray scattering, NR does not alter membrane structure, as proven by its successful application in studies of similar systems (35–38).

NR experiments were performed on the surface profile analysis reflectometer (SPEAR), a time-of-flight reflectometer at the Los Alamos National Laboratory Lujan Neutron Scattering Center (39). SPEAR receives neutrons from a polychromatic, pulsed (20 Hz) source that passes through a partially coupled liquid hydrogen moderator at 20 K to shift their energy spectra. Choppers and frame-overlap mirrors reduce the wavelength range of the neutrons to 2–16 Å. The wavelength,  $\lambda$ , and momentum of incident neutrons are related by the de Broglie relation,  $\lambda = h/p$ , where  $h$  is Planck's constant and  $p$  is the momentum of the neutron. By measuring the time it takes a neutron to travel the length of the instrument, the neutron's momentum, and therefore its wavelength, can be determined. During a NR experiment, neutrons impinge on a sample at a small angle,  $\theta$ , and the ratio of elastically scattered to incident neutrons is measured. This ratio is defined as the reflectivity,  $R$ , and is measured as a function of the momentum transfer vector,  $Q_z$ , where  $Q_z = 4\pi\sin[\theta]/\lambda$ . The incident neutron beam is collimated with a series of slits to create a footprint on the sample of  $\sim 20 \times 50$  mm. The coherent area of the neutron beam projected onto the sample is  $\sim 1 \times 100\text{ }\mu\text{m}$ , and the acquired data are averaged from the reflectivity from the coherent areas that make up the footprint. Because the average intensity over a large area is measured, reflectivity is sensitive to the surface coverage of the membrane. The reflectometry data presented here are multiplied by  $Q_z^{-4}$  to highlight deviations from the sharp decrease in reflectivity, as described by Fresnel's law:  $R\alpha Q_z^{-4}$  (40).

Analysis of specular reflectometry data provides information regarding the coherent scattering length density (SLD) distribution normal to the sample surface,  $\text{SLD}(z)$ , where  $z$  denotes the distance from the substrate. SLD is a value unique to a particular chemical composition and is the sum of the coherent scattering lengths of the constituent elements divided by the volume they occupy. It is important to note that the measured SLD values are absolute, because NR data are normalized to the incident

neutron intensity. To obtain a real-space interpretation of the scattering data,  $SLD(z)$ , a Fourier transform can be applied. Because only intensity and no phase information is collected, a unique Fourier transform between a single NR profile and its real-space interpretation does not exist (41,42). Therefore, modeling was employed to interpret the NR data.

The continuous function  $SLD(z)$  often can be well approximated by a number of layers, referred to as boxes, each with a constant SLD. Interlayer roughness can be taken into account using an error function centered at each interface (43). The incident neutron beam is refracted at each interface, and a theoretical NR curve can be calculated using the Parratt recursion formula (44). The measured and theoretical NR curves are compared, and using genetic optimization and the Levenburg-Marquardt nonlinear least-squares method, the best least-squares fit, corresponding to the lowest  $\chi^2$  value, is obtained (45). Details of our fitting philosophy are explained in Fig. S3.

By fitting the corresponding NR profiles, the SLD of each membrane was determined before and after the introduction of  $\beta$ -CD.  $\beta$ -CD might remove material from some membranes, which could result in the introduction of  $D_2O$  into regions previously occupied by membrane. The SLD of the membrane layer after removal of material ( $SLD_{after}$ ) is the sum of the SLD of  $D_2O$  ( $SLD_{D_2O}$ ) and the SLD of the membrane ( $SLD_{before}$ ), each weighted by their respective volume fractions in the membrane layer:  $SLD_{after} = \alpha(SLD_{D_2O}) + (1 - \alpha)(SLD_{before})$ , where  $\alpha$  is the volume fraction of  $D_2O$ . The volume fraction of  $D_2O$  is proportional to the amount of membrane removed.

## RESULTS AND DISCUSSION

Deposition surface pressure may play a critical role in the formation of the mixed SM/Chol membranes and their interaction with  $\beta$ -CD. To determine the effect of surface pressure, membranes of varying molar ratios of SM and Chol (100:0, 90:10, 67:33, 50:50, and 33:67) were deposited at 20, 30, and 40 mN/m, and the membrane structures were characterized before and after the introduction of  $\beta$ -CD. The interaction of  $\beta$ -CD with the membranes was independent of the deposition pressure except in the case of 50:50 membranes deposited at 40 mN/m. Therefore, all subsequent membranes characterized by NR were deposited at a surface pressure of 30 mN/m. Membranes are divided into two categories, those for which the global molar ratio was at or above the stable complexation ratio (no excess Chol) and those for which it was below the complexation ratio (excess Chol).

### Membranes with no excess Chol

Membranes at or above the stable complexation ratio are hypothesized to be composed of either pure complexes (global molar ratio of 67:33), complexes with excess SM (90:10), or pure SM (100:0). The initial structure of each membrane in  $D_2O$  was determined before introduction of  $\beta$ -CD. Exchanging the subphase of the solid-liquid cell from pure  $D_2O$  to 1 mM of  $\beta$ -CD in  $D_2O$  had no effect on the scattering from symmetric membranes (67:33, 90:10, 100:0). Fig. 1 shows representative NR data and an SLD profile for a symmetric 67:33 bilayer deposited at a surface pressure of 30 mN/m (Fig. S4 and Fig. S5 show scattering and SLD profiles for 90:10 and 100:0 bilayers).  $\beta$ -CD had no effect on these membranes, which suggests that it cannot remove pure SM or Chol that is complexed with SM. These results corroborate the hypothesis that  $\beta$ -CD is unable to complex double-chain phospholipids.

To probe the effect of starting membrane structure, an asymmetric membrane was created that had a global molar ratio of 67:33 (inner leaflet 100:0; outer leaflet 33:67). Although the outer leaflet was deposited with a proportion of Chol beyond the stable complexation ratio, introduction of  $\beta$ -CD had no effect on the scattering from this membrane (Fig. S6). We hypothesize that SM and Chol molecules were exchanged between the inner and outer leaflets and that eventually the membrane reorganized such that both leaflets had the same composition (homogenization) before  $\beta$ -CD addition. Considering all the molecules in the membrane, there is sufficient SM to complex all of the Chol, and we have shown that stable complexes are unaffected by  $\beta$ -CD. Membranes were characterized by NR within 1 h of deposition, which represents an upper bound for the membrane homogenization timescale. Table 1 reports the membranes unaffected by  $\beta$ -CD.

### Membranes with excess Chol

Symmetric membranes composed of 50:50 and 33:67 (~25% and ~50% excess Chol by mole fraction, respectively) were

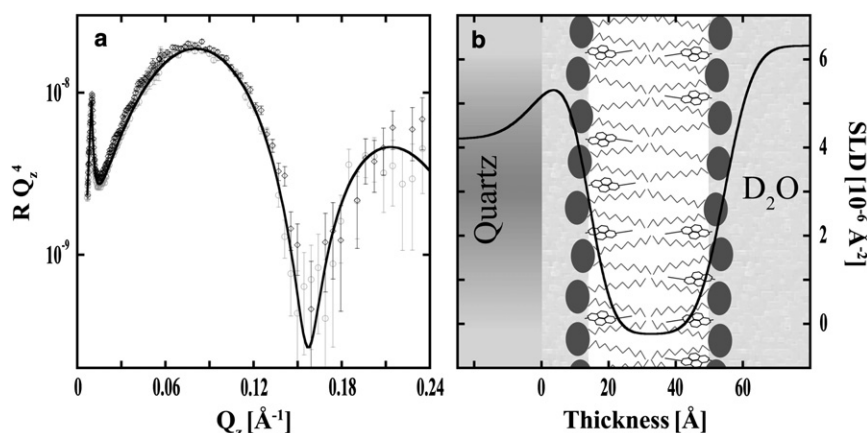
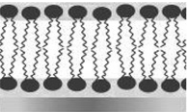
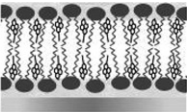
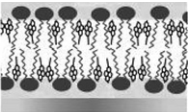
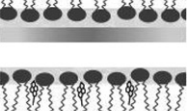
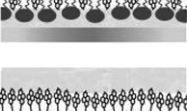
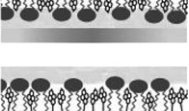
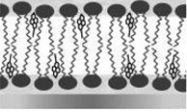
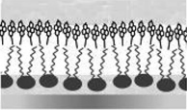
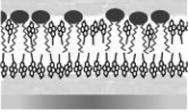
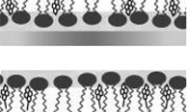
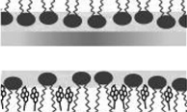

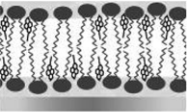
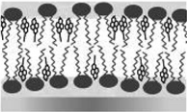
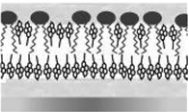
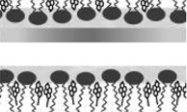


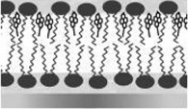



FIGURE 1 Analysis of the neutron scattering from a 67:33 SM/Chol bilayer deposited at a surface pressure of 30 mN/m. (a) The measurements before (black diamonds) and after (gray circles) the introduction of  $\beta$ -CD solution are shown, with the black line representing the fit. Error bars indicate 1 standard deviation (SD). (b) A real-space cartoon corresponding to the SLD profile (black line). The scattering from the system was unaffected by the introduction of  $\beta$ -CD.

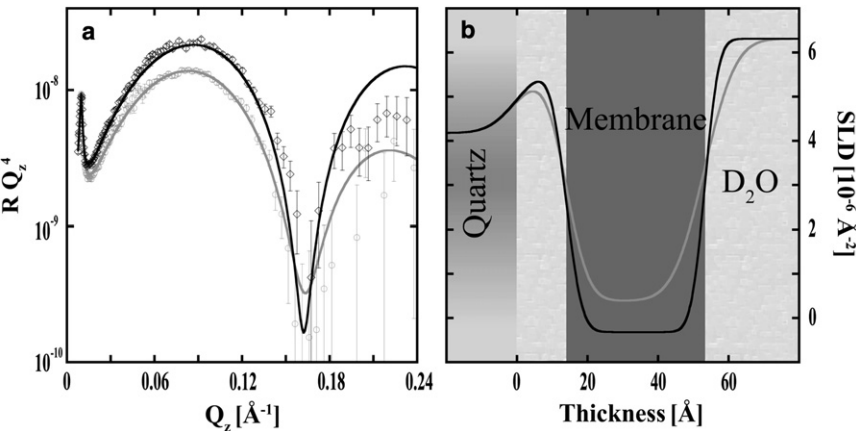
**TABLE 1** Change in surface coverage after introduction of  $\beta$ -CD for different initial membrane compositions

At or below the stable complexation ratio (no excess cholesterol)		Above the stable complexation ratio (excess cholesterol)			
		50:50 global molar ratio		33:67 global molar ratio	
Starting membrane structure	$\Delta$ Surface area	Starting membrane structure	$\Delta$ Surface Area	Starting membrane structure	$\Delta$ Surface area
100:0 	0 %	50:50 	$11 \pm 3$ %	33:67 	$22 \pm 3$ %
100:0 		50:50 		33:67 	
90:10 	0 %	Chol 	$11 \pm 3$ %	67:33 	$27 \pm 3$ %
90:10 		SM 		Chol 	
67:33 	0 %	33:67 	$8 \pm 3$ %	67:33 	$28 \pm 3$ %
67:33 		67:33 		dChol 	
33:67 	0 %				
100:0 					

All membranes were deposited at a surface pressure of 30 mN/m. dChol, deuterated Chol.

created to study the removal of excess Chol by  $\beta$ -CD. First, the interaction between 50:50 membranes and  $\beta$ -CD was studied qualitatively using fluorescence microscopy (see [Supporting Material](#)). The bilayer appeared uniformly red before introduction of  $\beta$ -CD because the Texas Red 1,2-dihexanoyl-*sn*-glycero-3-phosphoethanolamine (TR-DHPE) was distributed homogeneously ([Fig. S2 a](#)). No in-plane structure was apparent, because above a surface pressure of  $\sim 12$  mN/m, SM/Chol domains are too small to be resolved using optical methods (6). After addition of  $\beta$ -CD, dark regions, where there was no TR-DHPE, were observed ([Fig. S2 b](#)), indicating that the structure of the bilayer had been modified.

Fluorescence microscopy provides qualitative evidence that the structure of 50:50 membranes is modified by  $\beta$ -CD. To quantify the change in membrane structure, scattering from 50:50 membranes was compared first in the presence of  $D_2O$  and then in the presence of 1 mM  $\beta$ -CD solution. The scattering from these bilayers changes significantly after interaction with  $\beta$ -CD. Representative NR and SLD profiles from a symmetric 50:50 membrane are shown in [Fig. 2](#). The decrease in scattering amplitude suggests a decrease in surface coverage of the bilayer. Since we have shown that  $\beta$ -CD cannot remove SM or complexed Chol ([Fig. 1](#)), we associate the change in surface coverage with the removal



**FIGURE 2** Analysis of the neutron scattering from a 50:50 SM/Chol bilayer deposited at a surface pressure of 30 mN/m. (a) The measurements before (black diamonds) and after (gray circles) the introduction of the  $\beta$ -CD solution are shown, with error bars indicating 1 SD. (b) SLD profiles before (black line) and after (gray line) introduction of  $\beta$ -CD, with corresponding real-space cartoon. The amplitude of the scattering decreases (a) and the SLD of the membrane region increases (b), indicating that  $\beta$ -CD removed the uncomplexed Chol.



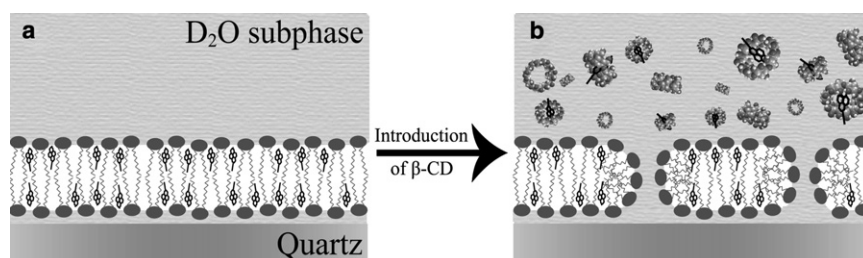


FIGURE 3 Cartoon depiction of a mixed SM/Chol bilayer before and after introduction of  $\beta$ -CD. (a) Initially, the bilayer is complete. (b) After  $\beta$ -CD is introduced, it removes Chol from the membrane and the bilayer subsequently reorganizes to hide the exposed hydrophobic tails of Chol and SM from the subphase. The resultant membrane layer has regions that are filled by the subphase.

of uncomplexed Chol. For the discussed neutron scattering experiments, the contrast existed mostly between the hydrogenated tails and the deuterated subphase. The tails of Chol and SM are mostly composed of carbon and hydrogen and therefore have low SLD values, about  $-0.30 \times 10^{-6} \text{ \AA}^{-2}$ . On the other hand,  $\text{D}_2\text{O}$  has a comparatively high SLD,  $6.3 \times 10^{-6} \text{ \AA}^{-2}$ . If  $\beta$ -CD removes uncomplexed Chol, the membrane will reorganize to hide the exposed hydrophobic tails of the remaining SM and Chol from the subphase and in the process will create regions in the bilayer that are subsequently filled by  $\text{D}_2\text{O}$  (Fig. 3). Once it reorganizes, the remaining membrane layer should have a higher SLD because of the averaging between the low SLD of the hydrogenated tails and the high SLD of the  $\text{D}_2\text{O}$  that occupies spaces created in the membrane (note the increase in SLD between  $\sim 14$  and  $52 \text{ \AA}$  in Fig. 2 b).

Two asymmetric membranes with the same 50:50 global molar ratio were created to investigate the effect of starting membrane structure on the removal of Chol by  $\beta$ -CD. One asymmetric membrane was composed of pure SM in the inner and pure Chol in the outer leaflet, and the second membrane was composed of 67:33 in the inner and 33:67 in the outer leaflet. Introduction of  $\beta$ -CD produced a similar decrease in surface coverage in the asymmetric bilayers compared to the symmetric 50:50 membranes (Fig. S7 and Fig. S8 show scattering and SLD curves of these asymmetric membranes). The changes in the surface area of 50:50 membranes after introduction of  $\beta$ -CD are summarized in Table 1.

The amount of Chol removed from 50:50 membranes was independent of starting structure, which provides further

evidence that the membrane homogenizes before  $\beta$ -CD is introduced. Membrane homogenization strongly suggests that the removal of Chol by  $\beta$ -CD is followed by membrane reorganization. For homogeneity to be maintained, Chol removal and subsequent membrane reorganization will continue until all excess Chol has been removed. Considering the area/molecule of the membranes' constituents ( $35$ ,  $37$ , and  $43 \text{ \AA}^2$  for Chol, stable complexes, and SM, respectively, at  $30 \text{ mN/m}$ ), the area occupied by excess Chol can be calculated. Uncomplexed Chol occupies  $\sim 25\%$  of the surface area of a 50:50 bilayer. However, the observed change in surface area of the membrane was  $\sim 11\%$ . The discrepancy in the observed and theoretical changes in surface coverage can be explained by membrane relaxation after removal of Chol. When Chol was removed and the membrane packing was no longer constrained, the area/molecule of the membrane constituents increased. For all membranes with a 50:50 global molar ratio, irrespective of starting structure, the introduction of  $\beta$ -CD produced a change in SLD of the membrane layer that was consistent with the removal of all excess Chol.

Bilayers composed of 33:67 (SM/Chol) were created to investigate how the amount of excess Chol affects final membrane surface coverage after introduction of  $\beta$ -CD. NR profiles corresponding to 33:67 membranes in  $\text{D}_2\text{O}$  and then in  $1 \text{ mM } \beta$ -CD solution were compared. For representative NR and SLD profiles from a symmetric 33:67 membrane, see Fig. 4 a. After introduction of  $\beta$ -CD, the decrease in scattering amplitude was greater for 33:67 membranes compared to 50:50 membranes, because the

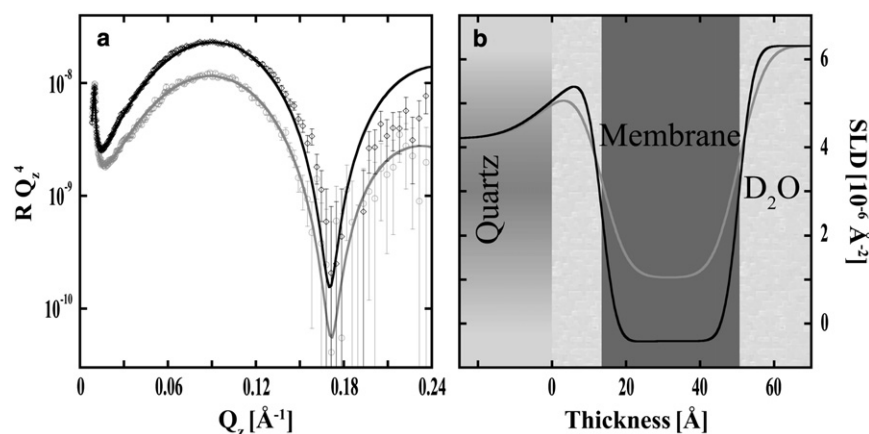


FIGURE 4 Analysis of the neutron scattering from a 33:67 SM/Chol bilayer. (a) Measurements are shown before (black diamonds) and after (gray circles) introduction of the  $\beta$ -CD solution, with error bars indicating 1 SD. (b) SLD profiles before (black line) and after (gray line) introduction of  $\beta$ -CD, with corresponding real-space cartoon. The amplitude of the scattering decreases (a) and the SLD of the membrane region increases (b), indicating that  $\beta$ -CD removed all uncomplexed Chol.

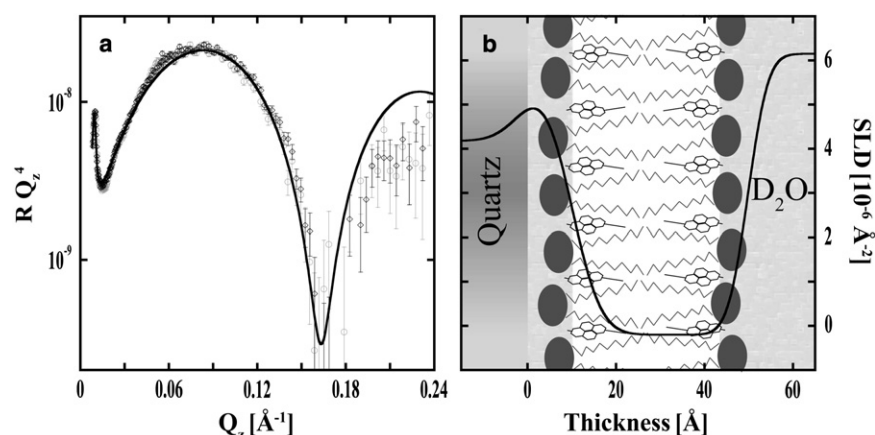


FIGURE 5 Analysis of the neutron scattering from a 50:50 SM/Chol bilayer deposited at a surface pressure of 40 mN/m. (a) The measurements before (black diamonds) and after (gray circles) the introduction of  $\beta$ -CD solution are shown, with the black line representing the fit. Error bars indicate 1 SD. (b) A real-space cartoon corresponding to the SLD profile (black line). The addition of  $\beta$ -CD had no effect on the scattering from the bilayer. The high deposition surface pressure and surface coverage of the bilayer could result in packing so tight that  $\beta$ -CD could not remove Chol.

33:67 bilayers contain more uncomplexed Chol. Similar results were observed for two asymmetric bilayers with the same global molar ratio (Fig. S9 and Fig. S10), consistent with the theory that asymmetric membranes homogenize before  $\beta$ -CD is introduced. The change in surface coverage for 33:67 membranes after introduction of  $\beta$ -CD suggests removal of all excess Chol and relaxation of the membrane. The changes in surface area of membranes with global molar ratios of 33:67 are presented in Table 1.

Surface pressure may influence the interaction between a SM/Chol membrane and  $\beta$ -CD. The interaction between  $\beta$ -CD and a symmetric 50:50 membrane deposited at 40 mN/m was unlike the effects observed involving 50:50 bilayers deposited at lower surface pressures. We were surprised to find that exchanging the subphase with the  $\beta$ -CD solution had no effect on the scattering (Fig. 5 a). Although the 50:50 bilayer contains more Chol than can be complexed with SM, both the high surface pressure and surface occupancy might have allowed the SM to hide the excess Chol. The SM and Chol in the bilayers deposited at lower surface pressure are packed less tightly than the constituents of the 50:50 bilayer deposited at 40 mN/m. The high surface pressure of the membrane could result in packing that was so tight it did not allow  $\beta$ -CD access to the Chol, similar to the umbrella model previously postulated (33).

## CONCLUSIONS

$\beta$ -CD is commonly used to remove Chol from cell lines to study various biological phenomena, such as lipid raft stability and cellular Chol depletion. However, its effect on different cellular constituents has remained unclear, which makes the interpretation of results from cell- $\beta$ -CD experiments problematic (19). We used systematic experiments involving membranes of known composition to show that  $\beta$ -CD is unable to remove complexed Chol. Using NR, membranes were characterized before and after exchanging the  $D_2O$  subphase with 1 mM of  $\beta$ -CD in  $D_2O$ . Scattering from bilayers composed of pure SM (100:0), 90:10, and 67:33 SM/Chol showed no change after

introduction of  $\beta$ -CD. This suggests that  $\beta$ -CD is unable to remove pure SM or complexed Chol. Both pure SM and 90:10 bilayers were completely unaffected by the introduction of  $\beta$ -CD, corroborating the hypothesis that  $\beta$ -CD is unable to complex double-chain phospholipids. Bilayers with global molar ratios of 50:50 and 33:67 contain a greater proportion of Chol than the stable SM/Chol complexation ratio;  $\beta$ -CD removed all excess Chol. Similar changes in surface coverage for symmetric and asymmetric membranes with the same global molar ratio strongly suggest that the membrane homogenizes before introduction of  $\beta$ -CD. The observed changes in surface coverage can be explained by in-plane relaxation of the membrane after Chol removal. It is interesting that the same effect was not seen in highly packed 50:50 bilayers deposited at a surface pressure of 40 mN/m. In this case, the neutron scattering was unaffected by the introduction of  $\beta$ -CD. We hypothesize that the tight packing of the membrane constituents does not allow  $\beta$ -CD access to the uncomplexed Chol.

## SUPPORTING MATERIAL

Ten figures are available at [http://www.biophysj.org/biophysj/supplemental/S0006-3495\(10\)00740-X](http://www.biophysj.org/biophysj/supplemental/S0006-3495(10)00740-X).

This work benefited from the use of the Lujan Neutron Scattering Center at Los Alamos Neutron Science Center, which was funded by the U.S. Department of Energy Office of Basic Energy Sciences and Los Alamos National Laboratory under Department of Energy contract DE-AC52-06NA25396.

## REFERENCES

1. Singer, S. J., and G. L. Nicolson. 1972. The fluid mosaic model of the structure of cell membranes. *Science*. 175:720–731.
2. Holthuis, J. C. M., and T. P. Levine. 2005. Lipid traffic: floppy drives and a superhighway. *Nat. Rev. Mol. Cell Biol.* 6:209–220.
3. Keller, S. L., W. H. Pitcher, ..., H. M. McConnell. 1998. Red blood cell lipids form immiscible liquids. *Phys. Rev. Lett.* 81:5019–5022.
4. Sackmann, E., editor. 1995. *Biological Membranes Architecture and Function*. Elsevier Science, Amsterdam.

5. Simons, K., and E. Ikonen. 1997. Functional rafts in cell membranes. *Nature*. 387:569–572.
6. Radhakrishnan, A., and H. M. McConnell. 1999. Condensed complexes of cholesterol and phospholipids. *Biophys. J.* 77:1507–1517.
7. Ratajczak, M. K., E. Y. Chi, ..., K. Kjaer. 2009. Ordered nanoclusters in lipid-cholesterol membranes. *Phys. Rev. Lett.* 103:028103.
8. Hanzal-Bayer, M. F., and J. F. Hancock. 2007. Lipid rafts and membrane traffic. *FEBS Lett.* 581:2098–2104.
9. Schütz, G. J., G. Kada, ..., H. Schindler. 2000. Properties of lipid microdomains in a muscle cell membrane visualized by single molecule microscopy. *EMBO J.* 19:892–901.
10. Stauffer, T. P., and T. Meyer. 1997. Compartmentalized IgE receptor-mediated signal transduction in living cells. *J. Cell Biol.* 139:1447–1454.
11. McIntosh, T. J., A. Vidal, and S. A. Simon. 2003. Sorting of lipids and transmembrane peptides between detergent-soluble bilayers and detergent-resistant rafts. *Biophys. J.* 85:1656–1666.
12. Slotte, J. P. 1999. Sphingomyelin-cholesterol interactions in biological and model membranes. *Chem. Phys. Lipids*. 102:13–27.
13. Wang, W., Y. J. Fu, ..., T. Efferth. 2009. Lipid rafts play an important role in the vesicular stomatitis virus life cycle. *Arch. Virol.* 154:595–600.
14. London, E., and D. A. Brown. 2000. Insolubility of lipids in triton X-100: physical origin and relationship to sphingolipid/cholesterol membrane domains (rafts). *Biochim. Biophys. Acta*. 1508:182–195.
15. Chen, X., R. Morris, ..., P. J. Quinn. 2007. The isolation and structure of membrane lipid rafts from rat brain. *Biochimie*. 89:192–196.
16. Meder, D., and K. Simons. 2006. Lipid rafts, caveolae and membrane traffic. In *Lipid Rafts and Caveolae: From Membrane Biophysics to Cell Biology*. C. J. Fielding, editor. Wiley, Weinheim, Germany.
17. Kilsdonk, E. P. C., P. G. Yancey, ..., G. H. Rothblat. 1995. Cellular cholesterol efflux mediated by cyclodextrins. *J. Biol. Chem.* 270:17250–17256.
18. Yancey, P. G., W. V. Rodriguez, ..., G. H. Rothblat. 1996. Cellular cholesterol efflux mediated by cyclodextrins. Demonstration of kinetic pools and mechanism of efflux. *J. Biol. Chem.* 271:16026–16034.
19. Zidovetzki, R., and I. Levitan. 2007. Use of cyclodextrins to manipulate plasma membrane cholesterol content: evidence, misconceptions and control strategies. *Biochim. Biophys. Acta*. 1768:1311–1324.
20. Szejtli, J. 1998. Introduction and general overview of cyclodextrin chemistry. *Chem. Rev.* 98:1743–1754.
21. Chou, T. H., and C. H. Chang. 2000. Thermodynamic behavior and relaxation processes of mixed DPPC/cholesterol monolayers at the air/water interface. *Colloids Surf. B Biointerfaces*. 17:71–79.
22. Ohvo-Rekilä, H., B. Ramstedt, ..., J. P. Slotte. 2002. Cholesterol interactions with phospholipids in membranes. *Prog. Lipid Res.* 41:66–97.
23. Ohvo, H., and J. P. Slotte. 1996. Cyclodextrin-mediated removal of sterols from monolayers: effects of sterol structure and phospholipids on desorption rate. *Biochemistry*. 35:8018–8024.
24. Christian, A. E., M. P. Haynes, ..., G. H. Rothblat. 1997. Use of cyclodextrins for manipulating cellular cholesterol content. *J. Lipid Res.* 38:2264–2272.
25. Rawlyer, A., and P. A. Siegenthaler. 1996. Cyclodextrins: a new tool for the controlled lipid depletion of thylakoid membranes. *Biochim. Biophys. Acta*. 1278:89–97.
26. Besenicar, M. P., A. Bavdek, ..., G. Anderluh. 2008. Kinetics of cholesterol extraction from lipid membranes by methyl- $\beta$ -cyclodextrin—a surface plasmon resonance approach. *Biochim. Biophys. Acta*. 1778:175–184.
27. Ohvo-Rekilä, H., B. Akerlund, and J. P. Slotte. 2000. Cyclodextrin-catalyzed extraction of fluorescent sterols from monolayer membranes and small unilamellar vesicles. *Chem. Phys. Lipids*. 105:167–178.
28. Puskás, I., and F. Csémpesz. 2007. Influence of cyclodextrins on the physical stability of DPPC-liposomes. *Colloids Surf. B Biointerfaces*. 58:218–224.
29. Asgharian, B., D. A. Cadenhead, and E. D. Goddard. 1988. The sequestering of surfactants from insoluble monolayers by  $\alpha$ -cyclodextrin,  $\beta$ -cyclodextrin and  $\gamma$ -cyclodextrin. *Colloids Surf.* 34:143–149.
30. Giocondi, M. C., P. E. Milhiet, ..., C. Le Grimallec. 2004. Use of cyclodextrin for AFM monitoring of model raft formation. *Biophys. J.* 86:861–869.
31. Mascetti, J., S. Castano, ..., B. Desbat. 2008. Organization of  $\beta$ -cyclodextrin under pure cholesterol, DMPC, or DMPG and mixed cholesterol/phospholipid monolayers. *Langmuir*. 24:9616–9622.
32. Ramstedt, B., and J. P. Slotte. 1999. Interaction of cholesterol with sphingomyelins and acyl-chain-matched phosphatidylcholines: a comparative study of the effect of the chain length. *Biophys. J.* 76:908–915.
33. Huang, J. Y., and G. W. Feigenson. 1999. A microscopic interaction model of maximum solubility of cholesterol in lipid bilayers. *Biophys. J.* 76:2142–2157.
34. Vaknin, D., M. S. Kelley, and B. M. Ocko. 2001. Sphingomyelin at the air-water interface. *J. Chem. Phys.* 115:7697–7704.
35. Callow, P., G. Fragneto, ..., M. J. Lawrence. 2009. Interaction of cationic lipid/DNA complexes with model membranes as determined by neutron reflectivity. *Langmuir*. 25:4181–4189.
36. Majewski, J., T. L. Kuhl, ..., G. S. Smith. 1997. Structure of phospholipid monolayers containing poly(ethylene glycol) lipids at the air-water interface. *J. Phys. Chem. B*. 101:3122–3129.
37. Smith, H. L., M. C. Howland, ..., J. Majewski. 2009. Early stages of oxidative stress-induced membrane permeabilization: a neutron reflectometry study. *J. Am. Chem. Soc.* 131:3631–3638.
38. Smith, H. L., M. S. Jablin, ..., J. Majewski. 2009. Model lipid membranes on a tunable polymer cushion. *Phys. Rev. Lett.* 102:228102.
39. <http://www.lansce.lanl.gov/lujan/instruments/SPEAR/index.html>. Accessed February 1, 2010.
40. Als-Nielsen, J. 1986. Synchrotron x-ray studies of liquid-vapor interfaces. *Physica A*. 140:376–389.
41. Berk, N. F., and C. F. Majkrzak. 1995. Using parametric B splines to fit specular reflectivities. *Phys. Rev. B Condens. Matter*. 51:11296–11309.
42. Majkrzak, C. F., and N. F. Berk. 1995. Exact determination of the phase in neutron reflectometry. *Phys. Rev. B Condens. Matter*. 52:10827–10830.
43. Nevot, L., and P. Croce. 1980. Characterization of surfaces by grazing x-ray reflection: application to study of polishing of some silicate-glasses. *Rev. Phys. Appl. (Paris)*. 15:761–779.
44. Parratt, L. G. 1954. Surface studies of solids by total reflection of x-rays. *Phys. Rev.* 95:359–369.
45. Nelson, A. 2006. Co-refinement of multiple-contrast neutron/X-ray reflectivity data using MOTOFIT. *J. Appl. Cryst.* 39:273–276.